

# Atom Optics with Magnetic Surfaces II: Microscopic Analysis of the “Floppy Disk” Mirror

I. G. Hughes <sup>a</sup>, P. A. Barton <sup>a</sup>, T. M. Roach <sup>b</sup>, and E. A. Hinds <sup>a,b</sup>

<sup>a</sup>*Sussex Centre for Optical and Atomic Physics,  
University of Sussex, Brighton, BN1 9QH, U.K.*

<sup>b</sup>*Physics Department, Yale University,  
P.O. Box 208120, New Haven, Connecticut 06520-8120*

- PACS numbers: 03.75.Be, 07.79.Pk, 32.80.Pj, 39.10.+j

## Abstract

In a recent experiment we studied cold rubidium atoms bouncing on a magnetic mirror made from a flexible computer disk with sinusoidal magnetisation. The motion was well described by a model in which the mirror was a perfect specular reflector, but complete agreement with the data required the reflecting surface to be slightly corrugated. Here we explore the physical origins of the corrugation both theoretically and experimentally.

First, we develop a theory relating the reflecting force on the atoms to the magnetisation of the mirror, taking into account the finite thickness of the magnetic film. We find that if the signal on the floppy disk is not harmonic the atoms appear to have been reflected from a corrugated surface, as observed in our recent experiment. Next, we describe magnetic force microscope measurements which allow us to determine the distortion on the disk and hence to quantify its effect on the reflected atoms. We show that recording nonlinearity is indeed a major cause of the mirror roughness. We also consider other sources of roughness and identify an important effect associated with the boundaries between recorded tracks. Agreement between our experiment and theory suggests that we have identified the limiting factors in real atom-optical element made from a floppy disk. At present the angular resolution of the mirror is approximately 35 mrad for atoms dropped from a height of 4 cm. We discuss how this can be improved to reach the level of 5 mrad or better.

## 1. Introduction

The field of atom optics has recently enjoyed spectacular growth, mainly due to the advance of techniques to manipulate atoms using laser light [1]. In our laboratory a related programme has been under way to manipulate atoms by means of their interaction with microstructured magnetic surfaces [2]. A recent paper from our group [3], henceforth called Paper I, described an experiment to bounce cold rubidium atoms on a spherical magnetic mirror made from a suitably magnetised flexible computer disk (“floppy disk”). Our analysis of the atomic motion showed that the mirror was a virtually perfect specular reflector, but that there were imperfections of the mirror surface which we tentatively ascribed to nonlinearities in the recording process. In this paper, the second of a series, we describe direct measurements of the microscopic magnetic properties of the same atomic mirror, which confirm the role of these nonlinearities and show that our physical understanding of

the mirror is substantially correct.

Section 2 presents a detailed discussion of the ideal magnetic mirror with sinusoidal magnetisation and also analyses the more general case in which two frequencies are present. In Section 3 we discuss the operation of a magnetic force microscope (MFM) and describe measurements which allowed us to determine the Fourier amplitudes of the magnetic field above our atomic mirror. The results of the MFM measurements are put into the theory in Section 4 and the predictions are compared with the results of Paper I. Finally, in Section 5, we summarise what has been learned from this microscopy and make a few remarks about the prospects for magnetic mirrors in the future.

## 2. Principles of the Magnetic Mirror

### 2.1. The ideal mirror

The principle of the magnetic mirror was first discussed by Vladimirkii [4] as a way to reflect cold neutrons and was later developed by

Opat *et al* [5] with a view to reflecting cold atoms. An atom in a magnetic field of magnitude  $B$  has the magnetic dipole interaction energy  $U = -\mu_z B$ , where  $\mu_z$  is the projection of its magnetic moment onto the field direction. Provided the magnetic field changes slowly enough (and it does for the cold atoms in our experiments) the magnetic moment follows the field adiabatically and the angle between them is constant. In this adiabatic regime the potential energy of the atom depends on the field magnitude  $B$ , but not its direction. The field of our atomic mirror increases near the surface and  $\mu_z$  is normally chosen to be negative so that the atom can be reflected by the Stern-Gerlach force  $\nabla\mu_z B$ . This is the basic principle. In this section we provide a more detailed mathematical description of the mirror than has been given before. We start with the case where the magnetisation of the mirror surface is exactly sinusoidal and then extend the discussion to allow for harmonic distortion of the magnetisation due to the nonlinearity of the recording process.

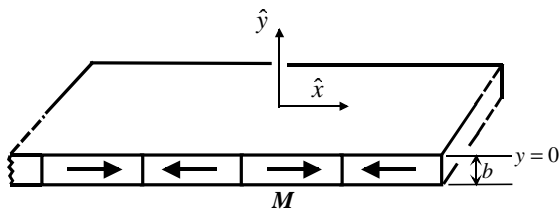


**Figure 1.** Schematic diagram of the mirror surface showing alternating magnetisation  $\mathbf{M}$  in the  $\hat{\mathbf{x}}$  direction. Also shown are the normal to the surface, which defines the  $\hat{\mathbf{y}}$  direction, the origin of the  $y$ -axis, and the thickness  $b$  of the magnetic layer.

The static field  $\mathbf{B}$  above a magnetic surface can be described by a scalar potential  $\phi$  related to the magnetisation  $\mathbf{M}(\mathbf{r}')$  within the material by equation (5.100) of Jackson's book [6]:

$$\phi(\mathbf{r}) = -\frac{\mu_0}{4\pi} \int_V \frac{\nabla' \cdot \mathbf{M}(\mathbf{r}')}{|\mathbf{r} - \mathbf{r}'|} d^3 r' + \frac{\mu_0}{4\pi} \oint_S \frac{\mathbf{n}' \cdot \mathbf{M}(\mathbf{r}')}{|\mathbf{r} - \mathbf{r}'|} d^2 r', \quad (1)$$

where  $V$  and  $S$  are the volume and surface of the material and  $\mathbf{n}'$  is the normal to the surface. For our atomic mirrors the direction of the magnetisation is primarily parallel or anti-parallel to one axis, which we take to define  $\hat{\mathbf{x}}$

as shown in figure 1. The surface of the mirror is flat with its normal  $\mathbf{n}'$  defining the  $\hat{\mathbf{y}}$  axis. With this geometry

$$\phi(\mathbf{r}) = -\frac{\mu_0}{4\pi} \int_V \frac{\partial M / \partial x'}{|\mathbf{r} - \mathbf{r}'|} d^3 r'. \quad (2)$$

An additional feature of the mirror is that the magnetisation is periodic with a repetition length  $\lambda$ , therefore it is convenient to expand the magnetisation in a Fourier series

$$M = \frac{1}{2} \sum_{n=0}^{\infty} M_n e^{inkx'} + \text{c.c.}, \quad (3)$$

in which  $k = 2\pi / \lambda$  and c.c. indicates the complex conjugate. Equation (2) then becomes

$$\phi(\mathbf{r}) = -\frac{\mu_0}{8\pi} \sum_n ink \int_V \frac{M_n e^{inkx'}}{|\mathbf{r} - \mathbf{r}'|} d^3 r' + \text{c.c.} \quad (4)$$

In general this integral cannot be evaluated analytically, however, Laplace's equation for  $\phi(\mathbf{r})$  together with the periodicity of  $\mathbf{M}$  impose a structure on the field of the form

$$\begin{pmatrix} B_x \\ B_y \end{pmatrix} = \mp \sum_n B_n e^{-nky} \begin{pmatrix} \cos(nkx + \delta_n) \\ \sin(nkx + \delta_n) \end{pmatrix}, \quad (5)$$

in which  $B_n$  is the field amplitude of the  $n^{\text{th}}$  harmonic at the surface of the mirror and  $\delta_n$  is the phase of the magnetisation defined by  $M_n = |M_n| e^{i\delta_n}$ . When the magnetisation is constant throughout the thickness  $b$  of the material, one finds that

$$B_n = \frac{1}{2} (1 - e^{-nkb}) \mu_0 |M_n|, \quad (6)$$

as we derive in Appendix A by direct integration of equation (4). This shows that the maximum field available to reflect atoms is only half the remanent field and that if the wavelength of the magnetisation is much greater than the thickness  $b$  of the magnetised layer, there is a further suppression given by the term in parentheses. These factors can be understood if we replace the magnetisation of the material by an effective surface current per unit width of  $\mathbf{M} \times \mathbf{n}'$ . The field due to the current on the front surface is  $\frac{1}{2} \mu_0 |\mathbf{M}|$ , but this is cancelled in part by the field from surface current flowing on the back. Finally, we note that each harmonic in equation (5) decreases exponentially with distance from the surface, the longest range being associated with the fundamental.

When the magnetisation is a pure sine wave, the magnitude  $B$  of the field is given by equation (5) as  $B_1 e^{-ky}$ , and for an atom whose mag-

netic moment along the field is  $\mu_\zeta$  the interaction energy is then

$$U = -\mu_\zeta B_1 e^{-ky}. \quad (7)$$

We see that for negative values of  $\mu_\zeta$  the interaction is repulsive and has flat equipotentials: in short, it is a mirror. To give a sense of the energy scales, we remark that a 15 G surface field is sufficient to reflect rubidium atoms in the ( $5S_{1/2}$   $F=3$ ,  $m_F=3$ ) ground state dropped from a height of 1 cm. In our atomic mirror, the surface field is roughly 230 G and the attenuation length  $1/k$  is approximately 2  $\mu\text{m}$ . For atoms dropped onto such a mirror, the reflecting potential is very steep compared with the gravitational one and the atom turns around in a very short distance. For the purposes of this paper, it is therefore a good approximation to regard the reflecting potential as a step at which the normal component of the atomic velocity is instantaneously reversed.

## 2.2. Nonlinear recording

When the magnetisation has more than one frequency component the equipotentials of the mirror are corrugated, producing a variation in the angle of reflection. Consider, for example, a mirror in which the magnetisation has just two Fourier components, the fundamental and the second harmonic. Then equation (5) gives

$$B^2 = B_1^2 e^{-2ky} + 2B_1 B_2 e^{-3ky} \cos(kx + \delta_2 - \delta_1) + B_2^2 e^{-4ky}. \quad (8)$$

If the atom is reflected at a large distance where  $ky \gg 1$ , the dominant term in equation (8) is the first one, which is generated by the fundamental, and the presence of the second harmonic has no significant effect on the operation of the mirror. Closer to the surface one cannot ignore the oscillating second term, but the last term remains negligible because  $B_2 e^{-ky} \ll B_1$  (unless we intentionally introduce a very strong second harmonic). Therefore

$$B \approx B_1 e^{-ky} \left[ 1 + \frac{B_2}{B_1} e^{-ky} \cos(kx + \delta_2 - \delta_1) \right]. \quad (9)$$

Thus the equipotential corresponding to a particular field magnitude is no longer flat. Its slope is given by

$$\vartheta = -\frac{\partial B / \partial x}{\partial B / \partial y} \approx -\frac{B_2 e^{-ky_0}}{B_1} \sin(kx + \delta_2 - \delta_1) \quad (10)$$

where  $y_0$  is the average height of the equipotential above the mirror, and we have continued to neglect small terms of order  $B_2 e^{-ky} / B_1$ . The amplitude of these ripples is equal to our small expansion parameter, which means that the mirror is flat to a first approximation and becomes increasingly so as the distance from the surface increases.

Atoms dropped from a height  $h$  at normal incidence onto the mirror penetrate to a depth where the magnetic potential energy  $-\mu_\zeta B_1 e^{-ky_0}$  is equal to the initial potential energy of the atom  $mgh$ . The angular variation of this maximum equipotential surface can be written according to equation (10) as

$$\Delta\vartheta = \frac{1}{\sqrt{2}} \left( \frac{B_2}{B_1} \right) \left( \frac{mgh}{-\mu_\zeta B_1} \right), \quad (11)$$

where  $\Delta\vartheta$  is the rms value of  $\vartheta$ . We note that this is proportional to the drop height  $h$  (provided  $\mu_\zeta$  is constant), so atoms dropped from a greater height will see a rougher mirror surface. Corrugations associated with a higher harmonic, say  $n$ , have a leading term which decays as  $e^{-(n-1)ky}$ . Higher harmonics are therefore even less important than the second harmonic except when the atom is very close to the mirror surface.

One might think of approximating the atomic trajectories by letting the atoms travel freely until they reach the corrugated equipotential at  $y_0$  where a fictitious hard surface reflects them by instantaneous reversal of the normal velocity. In this model the rms deviation of the reflected atoms is  $2\Delta\vartheta$ . However, this is not a good approximation because the atoms are in fact decelerated significantly in the region above  $y_0$  where the corrugation angle  $\vartheta$  is smaller, and therefore the angular diffusion of the reflected atoms is less than  $2\Delta\vartheta$ . In appendix B we show the surprisingly simple result that a hard surface whose corrugation angle is  $\vartheta_{\text{eff}} = 2\vartheta/3$  provides an excellent approximation to the real mirror.

## 3. Magnetic force microscopy of our mirror

Paper I describes the fabrication of an atom mirror from a floppy disk on which we had recorded a sine wave. In the experiment reported here we have used an MFM [7] to measure the field above this mirror surface

directly in order to determine the harmonic amplitudes  $B_n$  and calculate  $\Delta\vartheta$ . (See reference [8] for a recent review of magnetic microscopy). The sensor in our measurements consists of a sharp probe mounted on a silicon cantilever spring. The probe tip is coated with a 350 nm layer of cobalt-chromium alloy which is permanently magnetised in the (approximately) vertical direction. This material is chosen for the tip because it is magnetically hard and therefore provides a magnetic moment that is relatively independent of the strength of the field being measured. The interaction between the tip and the magnetic field changes the effective spring constant of the cantilever by an amount equal to the average force gradient and this is detected as a change in the resonant frequency of the tip as we now discuss.

### 3.1. Theory of the MFM response

Let us approximate the tip of the MFM as a harmonic oscillator of natural frequency  $\omega_0 = \sqrt{\kappa/m}$ , free to move in the  $y$  direction. Under the influence of a force component  $F_y$  the equation of motion is

$$m\ddot{y} = -\kappa y + F_y. \quad (12)$$

Making a Taylor expansion of the force  $F_y = F_0 + F'_y y + \dots$  we obtain the shifted resonant frequency

$$\omega = \sqrt{(\kappa - F'_y)/m} \equiv \omega_0 \left(1 - \frac{1}{2} F'_y / \kappa\right). \quad (13)$$

The neglect of quadratic variations in  $F_y$  over the tip and the assumption of a small frequency shift are both good approximations in our case. The MFM signal is proportional to the change in the resonant frequency, therefore it is essentially the derivative  $F'_y$  that the microscope measures.

The force on the tip is

$$\mathbf{F} = \int_V d^3r \nabla(\mathbf{M} \cdot \mathbf{B}), \quad (14)$$

where  $V$  is the volume of the tip and  $\mathbf{M}$  is its magnetisation. If we suppose that the tip is uniformly magnetised, then its magnetic moment  $\boldsymbol{\mu}$  is  $\mathbf{M}V$  and the force gradient generating the MFM signal is

$$F'_y = m \cdot \frac{1}{V} \int_V d^3r \frac{\partial^2 \mathbf{B}}{\partial y^2}. \quad (15)$$

For the periodic fields we are interested in,  $\boldsymbol{\mu} \cdot \mathbf{B}$  can be expanded as a Fourier series in which the  $n^{\text{th}}$  term is  $\mu B_n \sin(nk_0 x + \varphi_n) \exp(-nk_0 y)$ , (c.f. equation (5)). Here the phase  $\varphi_n$  depends on the direction of the tip magnetisation as well as the origin of the  $x$  co-ordinate. It follows that the  $n^{\text{th}}$  Fourier component of  $F'_y$  is

$$F'_y(nk_0) = (nk_0)^2 \frac{\mu B_n}{V} \int_V d^3r \sin(nk_0 x + \varphi_n) e^{-nk_0 y}. \quad (16)$$

If the tip is small compared with  $1/nk_0$ , the integrand is approximately constant over the integration volume and

$$F'_y(nk_0) = \xi_n B_n \sin(nk_0 x + \varphi_n) e^{-nk_0 y}, \quad (17)$$

where  $\xi_n$  is equal to  $\mu(nk_0)^2$ . Thus we can consider that the MFM maps out the field parallel to  $\boldsymbol{\mu}$  but with a sensitivity  $\xi_n$  that is different for each Fourier component.

When the size of the tip cannot be neglected, the volume average in equation (16) has to be carried out. One still finds, even for arbitrary tip geometry, that the force gradient on the MFM tip is given by a formula identical to equation (17). We do not present the derivation here because it is perfectly straightforward and rather tedious. Now  $x$  and  $y$  refer to the position of some reference point on the tip, for example the lowest point and the parameters  $\xi_n$  and  $\varphi_n$  include the effects of averaging over the tip volume. Moreover, the microscope signal continues to be described by equation (17) even when the direction of motion of the tip is not along  $y$  (i.e. not perpendicular to the surface) as we assumed in equation (12). So far we have used the parameters  $\xi_n$  and  $\varphi_n$ , evaluated at the harmonic frequencies  $nk_0$ , to describe the interaction between the MFM tip and a particular sample. More generally however, we require continuous functions  $\xi(k)$  and  $\varphi(k)$  to analyse the interaction of the same tip with different samples. Once these are known, it is possible to reconstruct the field above any surface from a Fourier analysis of the MFM scans provided the magnetisation is periodic and along  $x$ .

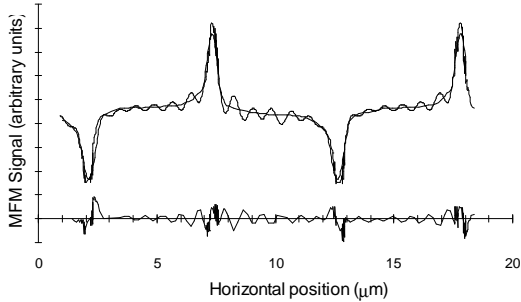


**Fig. 2.** MFM signal recorded 25 nm above a hard disk with square-wave magnetisation. Superimposed on this is the theoretical function given in equation 18 with fitting parameters  $C\xi_n$  and  $\phi_n$  chosen to minimise  $\chi^2$ . The fast oscillations in this curve are due to the truncation of equation 18 at  $n = 13$ . The residuals of the fit are also shown.

This point seems not to have been noted in the MFM literature to date [9, 10, 11, 12]. This idea can also be used to analyse surfaces magnetised along the  $z$  direction. In addition, one may be able to extend it to more general cases in which the magnetisation is not constrained to one direction, but that is beyond the scope of this article.

### 3.2. MFM Measurements

Following the ideas developed above, we first set about determining the functions  $\xi$  and  $\phi$  for the particular MFM tip used to measure the field above our magnetic mirror. This was done by scanning the tip at a height of 25 nm above a hard disk which had a square wave magnetisation of wavelength  $10.5 \mu\text{m}$ . On the basis of equations (17) and (6), we expect this signal to have the form

$$\text{MFM signal} = C \sum_{\text{odd } n} \xi_n (1 - e^{-nk_0 b}) \cdot \frac{1}{n} \sin[nk_0 x + \phi_n] e^{-nk_0 y}. \quad (18)$$

Here  $C$  incorporates all the constant factors in the MFM sensitivity,  $b = 1 \mu\text{m}$  is the thickness of the magnetic layer on the hard disk, and we have used the fact that the Fourier amplitudes of a square wave are  $1/n$  for odd  $n$ . Figure 2 shows the signal from approximately 200 MFM scans in the  $x$ -direction, representing an average over some  $10 \mu\text{m}$  in the  $z$ -direction. Also shown is a least-squares fit of equation (18) to this curve, keeping terms up to  $n = 13$  which span the range of wavevectors

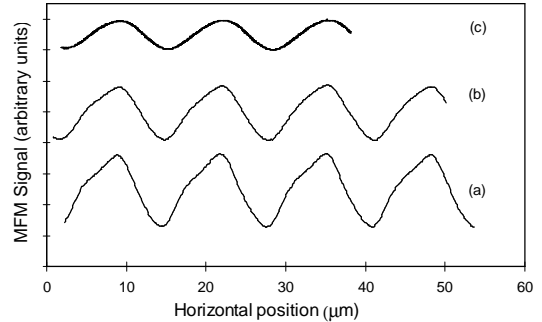


**Fig. 3.** MFM signals recorded above our floppy disk magnetic mirror at three different heights indicated by (a) (b) (c), corresponding to 0.5, 1.0, and  $2.0 \mu\text{m}$ . The three curves are on the same scale, but are offset vertically for clarity.

$0.6 - 7.8 \mu\text{m}^{-1}$ . The fitted curve has some high frequency oscillations due to the truncation of the series, but it is evident from the residuals that the experimental signal is indeed well described by equation (18). We also tried a fit in which even harmonics were allowed and in this way we found empirically that they were indeed absent or at least indistinguishable from the noise.

The values of  $\xi_n$  were found to be almost constant. This clearly indicates that the tip is not small on our scale because  $\xi_n \propto n^2$  for a tip of negligible size. In fact, for a hollow pyramid of small apex angle and height  $H \gg 1/k$  it can be shown by carrying out the integral in equation (16) that  $\xi(k)$  has the constant value  $2\mu/H^2$ , therefore our experimental result is not entirely surprising. Having calibrated  $\xi(k)$ , we were ready to scan the field above the atomic mirror to determine its Fourier amplitudes  $B_n$ .

Figure 3 shows MFM scans across the mirror taken at three fixed heights,  $y = 0.5, 1.0,$  and  $2.0 \mu\text{m}$  above the surface of the floppy disk. The first point to notice is that the field at a height of  $2.0 \mu\text{m}$  (slightly less than the closest approach of the most energetic atoms studied in Paper I) is essentially a pure sine wave, which implies that the equipotential for the atom-mirror interaction is flat, as predicted by the theory developed in Section 2. Of course, our mirror is not infinite, but one is not surprised to find that the theory works well because the number of oscillation periods is approximately 1400 (see reference [13] for a

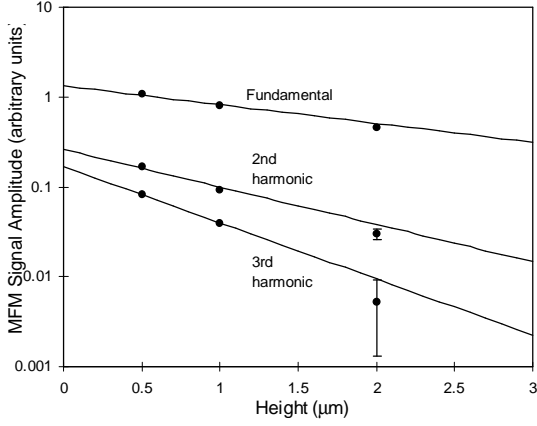


**Fig. 4.** Data points show the first three harmonics of the MFM signal as a function of height above our magnetic mirror. Lines are fits to the form  $a_n(0)\exp(-nk_0y)$  in which the only free parameters are the three values of  $a_n(0)$ .

discussion of end effects due to a small number of finite elements).

In order to explore the small distortions noted in Paper I, we fitted each scan to the function

$$\sum_{n=1}^3 a_n \sin(nk_0x + \phi_n)$$

to determine the amplitudes of the three leading Fourier components at that particular height. (Here  $k_0$  now refers to the periodicity of the mirror, not the calibration square wave). According to equation (17), each coefficient  $a_n$  should vary with height as  $a_n(0)\exp(-nk_0y)$ . Our values of  $a_n$  are plotted in figure 4 together with curves of this form, in which the three amplitudes at zero height,  $a_n(0)$ , are the fitting parameters. The fit demonstrates that the decay of each Fourier component with height is well described by the exponential factor  $\exp(-nk_0y)$ . Taking into account the frequency-dependent sensitivity of the MFM, we obtain the ratios of the field amplitudes at the surface by the relation

$$\frac{B_n}{B_1} = \frac{a_n(0)/a_1(0)}{\xi_n/\xi_1}. \quad (19)$$

We find that in our mirror the ratio of second and third harmonics to first are  $B_2/B_1=0.20(2)$  and  $B_3/B_1=0.14(2)$ . It is not surprising that the magnetic material responded nonlinearly to our sinusoidal input because the floppy disk is designed for digital applications and because we drove the magnetic material quite hard in order to achieve a large magnetisation. However, we expected

the second harmonic amplitude to be small on the grounds of symmetry and this is evidently not the case. At present we do not understand the cause of this, but it is not an artefact of our MFM technique.

#### 4. Comparison with the results of Paper I

By a straightforward extension of the discussion leading up to equation (11), one can show that the rms angular variation  $\Delta\vartheta$  of the equipotentials with energy  $mgh$  for a mirror such as ours with both second and third harmonic distortions should be given by

$$(\Delta\vartheta)^2 = \frac{1}{2} \left[ \frac{B_2}{B_1} \left( \frac{mgh}{\mu_\zeta B_1} \right) \right]^2 + \frac{1}{2} \left[ \frac{2B_3}{B_1} \left( \frac{mgh}{\mu_\zeta B_1} \right) \right]^2. \quad (20)$$

As we discuss in Appendix B, it is an excellent approximation to replace the mirror by an equivalent hard reflecting surface with a smaller rms angular variation given by

$$(\Delta\vartheta_{\text{eff}})^2 = \frac{1}{2} \left[ \frac{2}{3} \frac{B_2}{B_1} \left( \frac{mgh}{\mu_\zeta B_1} \right) \right]^2 + \frac{1}{2} \left[ \frac{16}{15} \frac{B_3}{B_1} \left( \frac{mgh}{\mu_\zeta B_1} \right) \right]^2. \quad (21)$$

In the experiment described in Paper I, rubidium atoms in the  $F=3$ ,  $m_F=3$  state were dropped from various heights  $h$  onto this mirror and values for  $\Delta\vartheta_{\text{eff}}$  were determined from a study of the atomic motion. We are now in a position to compare those values with the prediction of equation (21). When the various constants are replaced by their specific values in our experiment, we find that the third harmonic contribution is small for the heights up to 40.5 mm used in Paper I. Therefore equation (21) may be approximated by

$$\Delta\vartheta_{\text{eff}} = 0.60(7)h \left[ 1 + 2.5(6) \times 10^{-5} h^2 \right] \quad (22)$$

where  $\Delta\vartheta_{\text{eff}}$  is in mrad and  $h$  is in mm.

The data points in figure 5 are the values of  $\Delta\vartheta_{\text{eff}}$  measured in Paper I, while the shaded region shows the one standard deviation range of values deduced from our MFM measurements as encapsulated in equation (22). It is evident that the nonlinearity of the recording is indeed a major cause of the mirror roughness detected in Paper I. However, there is also a

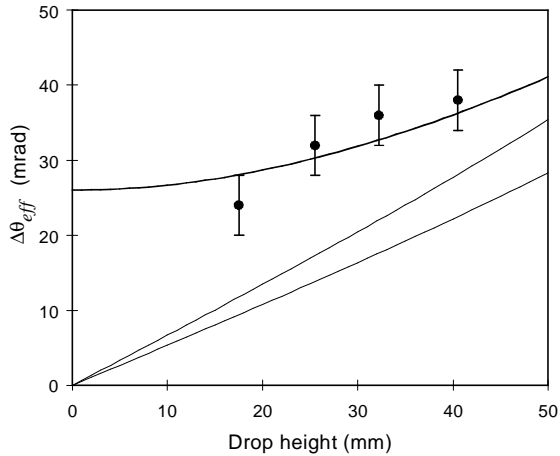


**Fig. 5.** Data points show the rms angular variation  $\Delta\vartheta_{\text{eff}}$  of the effective hard mirror surface as determined from the motion of bouncing atoms in Paper I. The shaded region shows the contribution to  $\Delta\vartheta_{\text{eff}}$  due to recording nonlinearity, deduced from the MFM measurements presented here. The solid line shows the combined effect of recording nonlinearity and discontinuities at the track boundaries.

substantial excess which is not explained by the magnetic corrugations due to harmonics of the field. We now consider possible causes of this.

Since the MFM scans at a fixed height above the surface of the floppy disk, one obvious possibility for the cause of the excess roughness is a variation in the height of the magnetic layer. In order to check this, we studied the floppy disk under an atomic force microscope (AFM) [14]. Figure 6 shows the profile of a typical line in the scan. Over a  $100\ \mu\text{m}$  square region, the standard deviation of the height is 22 nm and the maximum deviation from the mean is 100 nm. The topography of the equipotential at average height  $y_0$  should follow that of the underlying surface averaged over an area of order  $y_0 \times y_0$ . With this averaging procedure we used the AFM image to estimate the height variation and hence the rms angular variation of equipotentials  $2\ \mu\text{m}$  and  $4\ \mu\text{m}$  above our magnetic mirror. The results of this simple model are  $\Delta\vartheta = 7\ \text{mrad}$  at height  $2\ \mu\text{m}$  (drop height 64 mm) and  $\Delta\vartheta = 4\ \text{mrad}$  at height  $4\ \mu\text{m}$  (drop height 26 mm). These are not large enough to explain the excess angular variation observed in the atom bouncing experiment because they should be added in quadrature to the  $\Delta\vartheta$  caused by harmonics.

We think it is more likely that the excess roughness is caused by the boundaries between adjacent tracks of the magnetic recording.

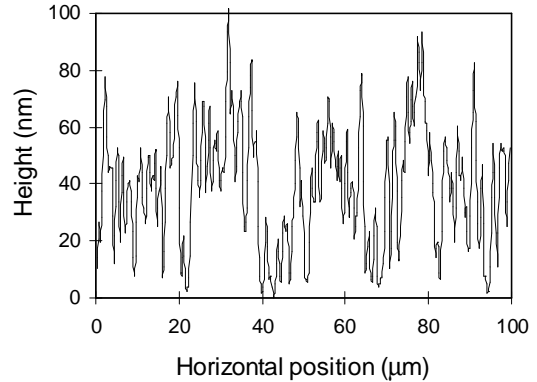


**Fig. 6.** Typical atomic force microscope scan across the surface of the floppy disk.

Along each boundary there is a region of width  $\sim \lambda$  where the field is distorted because the sine waves on the two tracks are not in phase with each other. In these regions, which cover approximately 0.03 of the mirror surface, there are strong angular variations of the magnetic equipotentials and atoms which land there are deflected through large angles. The angular variations reported in Paper I and shown as data points in figure 5 include this effect of the boundaries: our measurement did not distinguish the few atoms which suffer large deflections from the majority which have small deflections. Both can be incorporated into the theory by adding a constant angle, expected to be of order 0.03 rad, in quadrature with the corrugation caused by nonlinearity of the recording. The solid line in figure 5 shows this modified theory with a 26 mrad constant term as determined by a least-squares fit. This model is completely compatible with our data, and suggests that there are no other significant causes of non-specular reflection.

## 5. Summary and future prospects

We have developed a theory to describe the equipotentials of the Zeeman interaction above the surface of a magnetic mirror, which takes into account the finite thickness of the magnetic layer and the anharmonicity of the recording. We have also devised a method by which magnetic force microscopy can be used to determine the Fourier components of the mirror's magnetisation and used it to characterise the atom-optical properties of the mirror according to our theory.

Our measurements have shown that the equipotentials of the mirror are essentially flat and decrease exponentially as expected from the

theory. There is some spread in the angle of reflection of the atoms due to a corrugation of the reflecting surface caused by the presence of more than one frequency in the magnetisation of the surface. Additional angular spread is caused by the distortion of the equipotential surfaces at the boundaries between tracks. At present, these effects limit the optical quality of the mirror by restricting the angular resolution to a few tens of milliradians for atoms dropped from heights of a few centimetres.

There are two obvious ways to improve the performance of floppy disk mirrors in the future, both related to the way the signal is recorded. (i) It should be possible to reduce the amplitudes of the higher harmonics of the magnetisation recorded by an appropriate distortion of the input waveform. (ii) In order to avoid discontinuities at the boundaries, the tracks can be phase-locked to a reference track, ensuring that the loci of maxima and minima are radial. With these improvements one can hope to reach the 5 mrad level and we may well be able to do much better than that.

An alternative approach might be to use a magnetic material with a stronger remanent field so that the atoms are reflected at a larger distance from the surface where we have demonstrated that the higher harmonics have less effect. On both these counts the use of magnetic audio tape is attractive: the maximum field is of order 1 kG and the recording technology is carefully designed to optimise linearity. Of course, the synchronisation of tracks would be required here as well.

In devices for physical optics one needs to preserve the phase of the de Broglie wave front and it is necessary to consider the height variation of the surface. We know from our AFM image that the rms surface roughness is 22 nm. Using the simple model described in Section 4, we find that the equipotential 4  $\mu\text{m}$  above the surface has an rms roughness of order 12 nm. Since this is approximately equal to the de Broglie wavelength of a rubidium atom dropped from 1 cm, the prospects for a diffraction grating look good, particularly at grazing incidence angles. Other considerations related to the possibility of physical optics have been discussed by Opat *et al* [5].

## Acknowledgements

We are indebted to P. Grundy and D. Lord who made the MFM scans for us and to Mal-

colm Boshier for his assistance in the data analysis and several valuable discussions. This work was supported by the EPSRC and by the University of Sussex.

## Appendix A

This appendix fills in the steps connecting equations (4), (5) and (6). When the magnetisation is uniform throughout the thickness  $b$  of the medium, equation (4) reduces to

$$\phi(\mathbf{r}) = -\frac{\mu_0}{8\pi} \sum_{n=0}^{\infty} \text{inkM}_n I + \text{c.c.}, \quad (23)$$

in which  $I$  is the following integral over the magnetised volume

$$I = \int_V \frac{e^{i\mathbf{nkx}'}}{|\mathbf{r} - \mathbf{r}'|} d^3\mathbf{r}'. \quad (24)$$

Writing the Cartesian components of  $\mathbf{r} - \mathbf{r}'$  as  $(u, v, w)$ , this becomes

$$I = e^{i\mathbf{nkx}} \int_{-\infty}^{\infty} du \int_y^{y+b} dv \int_{-\infty}^{\infty} dw \frac{e^{-i\mathbf{nk}(v^2 + w^2)}}{(u^2 + v^2 + w^2)^{1/2}}. \quad (25)$$

The integral over  $u$  is symmetric therefore only the cosine term from the exponential survives. Now equations 3.754#2, 6.596#3 and 8.469#3 of reference [15] give

$$\int_{-\infty}^{\infty} du \frac{\cos(nku)}{(u^2 + v^2 + w^2)^{1/2}} = 2K_0[\text{nk}(v^2 + w^2)]$$

$$\int_0^{\infty} K_0[\alpha(x^2 + z^2)] dx = \left(\frac{z\pi}{2\alpha}\right)^{1/2} K_{-1/2}(\alpha z) \quad (26)$$

$$K_{-1/2}(\text{nk}v) = \left(\frac{\pi}{2\text{nk}v}\right)^{1/2} e^{-\text{nk}v}$$

where  $K$  is a Bessel function of imaginary argument. These lead from equation (25) to the result

$$I = \frac{2\pi}{(\text{nk})^2} e^{i\mathbf{nkx}} (1 - e^{-\text{nk}b}) e^{-\text{nk}y}. \quad (27)$$

The combination of equations (23) and (27) gives

$$\phi(\mathbf{r}) = -\frac{1}{2} \sum_{n=0}^{\infty} \frac{iB_n}{\text{nk}} e^{-\text{nk}y} e^{i(\text{nk}x + \delta_n)} + \text{c.c.}, \quad (28)$$

where, as we cite in equation (6),

$$B_n = \frac{1}{2} \mu_0 |M_n| (1 - e^{-\text{nk}b}). \quad (29)$$

The components of the field are therefore

$$B_x = -\frac{\partial \phi}{\partial x} = -\sum_{n=0}^{\infty} B_n e^{-\text{nk}y} \cos(\text{nk}x + \delta_n) \quad (30)$$

and

$$B_y = -\frac{\partial \phi}{\partial y} = \sum_{n=0}^{\infty} B_n e^{-\text{nk}y} \sin(\text{nk}x + \delta_n), \quad (31)$$

which is the result given in equation (5).

## Appendix B

This appendix relates the soft potential of the floppy disk mirror to an equivalent hard mirror.

### B1. First and second harmonics

We take as our starting point the equations of motion derived from equation (9), keeping only the leading terms:

$$\begin{aligned} m \frac{d^2 y}{dt^2} &= -\mu_\zeta B_1 k e^{-ky} \\ m \frac{d^2 x}{dt^2} &= -\mu_\zeta B_2 k \sin(kx) e^{-2ky} \end{aligned} \quad (32)$$

Naturally, we neglect the gravitational acceleration which has no appreciable effect while the atom is in the field of the mirror. Integration of the first equation above gives

$$v_y(t) = \pm v_0 \sqrt{1 - e^{-k(y-y_0)}} \quad (33)$$

where  $v_0$  is the initial velocity (i.e.  $-\sqrt{2gh}$  for a drop height  $h$ ) and  $y_0$  is the distance of closest approach. When we integrate once again we find the height as a function of time is given by

$$e^{-k(y-y_0)} = \sec^2 h^2 (t - t_0) / \tau, \quad (34)$$

where  $t_0$  is the time at the moment of closest approach and  $\tau = 2 / kv_0$  characterises the time of interaction between the atom and the mirror. For completeness we note that the time-dependence of the perpendicular velocity is

$$v_y(t) = -v_0 \tanh_0(t - t_0) / \tau \quad (35)$$

The  $x$ -component of velocity is found by substituting equation (34) into equation (32):

$$\begin{aligned} m \frac{dv_x}{dt} &= -\mu_\zeta B_2 k e^{-2ky_0} \\ &\cdot \sin(kx) \sec^4 h^2 (t - t_0) / \tau \end{aligned} \quad (36)$$

In general, this does not have a simple analytical solution, however we are interested in the particular cases where  $v_x \ll v_0$ . In these cases  $v_x \tau \ll \lambda$  and then the factor  $\sin(kx)$  is effectively a constant  $\sin(kx_0)$ , where  $x_0$  identifies the point of impact on the mirror. The angle of deviation from specular reflection is determined by the change in  $v_x$  resulting from the reflection, and is found by integrating equation (36) to be

$$\begin{aligned} \frac{\Delta v_x}{v_0} &= -\frac{\mu_\zeta B_2 k e^{-2ky_0} \sin(kx_0) 4\tau}{mv_0 3} \\ &= \frac{4}{3} \frac{B_2}{B_1} \left( \frac{mgh}{-\mu_\zeta B_1} \right) \sin(kx_0). \end{aligned} \quad (37)$$

We take the rms value of this and divide by 2 to obtain  $\Delta\vartheta_{\text{eff}}$ , the angular variation of the equivalent hard reflecting surface.

$$\Delta\vartheta_{\text{eff}} = \frac{2}{3\sqrt{2}} \frac{B_2}{B_1} \left( \frac{mgh}{-\mu_\zeta B_1} \right). \quad (38)$$

This is precisely 2/3 of  $\Delta\vartheta$ , the angular variation of the equipotential at  $y_0$  which is given in the text by equation (11). This factor is the main result we wish to show. In the course of deriving it, we have made a succession of reasonable approximations. In order to check that the net effect remains a good approximation we have compared equations (37) and (38) with a numerical calculation of the exact atomic trajectories. In this complete calculation the angles of deviation are indeed sinusoidal in  $x_0$  within a few percent and their variation is correctly characterised by our  $\Delta\vartheta_{\text{eff}}$  hard mirror approximation to better than 1%.

### B2. Higher harmonics

In the presence of higher harmonics the interference between the fundamental and the  $n^{\text{th}}$  harmonic leads to an additional acceleration in the  $x$  direction. The leading term is

$$\begin{aligned} m \left( \frac{dv_x}{dt} \right)_n &= -(n-1) \mu_\zeta B_n k e^{-2nky_0} \\ &\cdot \sin(n-1)kx \sec^{2n} h^2 (t - t_0) / \tau \end{aligned} \quad (39)$$

which is a simple extension of equation (36). A repetition of the analysis given above eventually yields an angular variation of the equivalent hard reflecting surface of

$$\begin{aligned} (\Delta\vartheta_{\text{eff}})_n &= \\ \frac{1}{\sqrt{2}} (n-1) &\left( \frac{B_n}{B_1} \right) \left( \frac{mgh}{-\mu_\zeta B_1} \right)^{n-1} \frac{(2n-2)!!}{(2n-1)!!}. \end{aligned} \quad (40)$$

This is to be compared with the angular variation at spatial frequency  $(n-1)k$  of the equipotential at  $y_0$

$$(\Delta\vartheta)_n = \frac{1}{\sqrt{2}}(n-1) \left( \frac{B_n}{B_1} \right) \left( \frac{mgh}{-\mu_\zeta B_1} \right)^{n-1}. \quad (41)$$

Once again we find that  $\Delta\vartheta_{\text{eff}}$  is related to  $\Delta\vartheta$  by a simple numerical factor, specifically  $(2n-2)!!/(2n-1)!!$ . For the particular case of  $n=2$  we recover the factor of  $2/3$  derived above. In the case of our mirror we wish to include both  $n=2$  and  $n=3$  and the variations  $(\Delta\vartheta_{\text{eff}})_2$  and  $(\Delta\vartheta_{\text{eff}})_3$  must be added in quadrature. This is how we arrived at the total angular variation given in equation (21) of the text.

## References

- 1 *Quantum Semiclass. Opt.* 1996 **8** Special issue on Atom Optics.
- 2 Roach T M, Abele H, Boshier M G, Grossman H L, Zetie K P and Hinds E A 1995 *Phys. Rev. Lett.* **75** 629.
- 3 Hughes I G, Barton P A, Roach T M, Boshier M G and Hinds E A 1996 to appear in *J.Phys.B*.
- 4 Vladimirskiĭ V V 1961 *Sov. Phys. JETP* **12** 740.
- 5 Opat G I, Wark S J and Cimmino A 1992 *Appl. Phys. B* **54** 396.
- 6 Jackson J D 1975 *Classical Electrodynamics* (Wiley and sons, New York).
- 7 Measurements performed by the EPSRC facility in Salford University using a Digital Instruments Inc. Dimension 3000 Scanning Probe Microscope used in *lift mode*.
- 8 Dahlberg E D and Zhu J-G 1995 *Physics Today*, April Issue p. 34.
- 9 Wadas A and Grutter P 1989 *Phys. Rev. B* **39** 12013
- 10 Hartmann U 1990 *J. Vac. Sci. Technol. A* **8** 411.
- 11 Rugar D, Mamin H J, Guethner P, Lambert S E, Stern J E, McFadyen I and Yogi T 1990 *J.Appl. Phys.* **68** 1169.
- 12 Wright C D and Hill E W 1996 *Appl. Phys. Lett.* **68** 1726.
- 13 Sidorov A I, McLean R J, Rowlands W J, Lau D C, Murphy J E, Walkiewicz M, Opat G I and Hannaford P 1996 *Quantum Semiclass. Opt.* **8** 713.
- 14 Measurement performed by the EPSRC facility in Salford University using a Digital Instruments Inc. Dimension 3000 Scanning Probe Microscope used in *tapping mode*.
- 15 Gradshteyn I S and Ryzhik I M 1980 *Tables of Integrals, Series and Products*, (Academic Press).